Hyperfine-structure study in the P sequence of 23 Na using quantum-beam spectroscopy

Grundevik, P; Lundberg, Hans; Martensson, A-M; Nystrom, K; Svanberg, Sune

Published in:
Journal of Physics B: Atomic and Molecular Physics

DOI:
10.1088/0022-3700/12/16/012

1979

Hyperfine-structure study in the P sequence of ^{23}Na using quantum-beam spectroscopy

1979 J. Phys. B: At. Mol. Phys. 12 2645

(http://iopscience.iop.org/0022-3700/12/16/012)

J. Phys. B: Atom. Molec. Phys., Vol. 12, No. 16, 1979. Printed in Great Britain

Hyperfine-structure study in the P sequence of ^{23}Na using quantum-beat spectroscopy

P Grundevik, H Lundberg, A-M Mårtensson, K Nyström and S Svanberg
Department of Physics, Chalmers University of Technology, S-402 20 Göteborg, Sweden

Received 28 December 1978, in final form 8 February 1979

Abstract. We have used the quantum-beat method to study hyperfine structure in the $5^2P_{3/2}$ and $6^2P_{3/2}$ states of ^{23}Na. A pulsed dye laser, frequency-doubled into the UV region, was used to excite sodium atoms abruptly in a beam. The fluorescent light was recorded with a fast transient digitiser, interfaced to a micro-computer. For the magnetic-dipole and the electric-quadrupole interaction constants a and b we obtained: $a(5^2P_{3/2}) = 2{\cdot}64(1)$ MHz, $b(5^2P_{3/2}) = 0{\cdot}38(3)$ MHz, $a(6^2P_{3/2}) = 1{\cdot}39(1)$ MHz and $b(6^2P_{3/2}) = 0{\cdot}21(2)$ MHz. Theoretical calculations using many-body perturbation theory were performed for the entire P sequence measured so far, taking polarisation and correlation effects into account separately. Very good agreement between experimental and theoretical values was obtained.

1. Introduction

Until recently, hyperfine-structure (HFS) studies in excited sodium states were limited to the low-lying $3^2P_{3/2}$, $3^2P_{1/2}$ and $4^2P_{3/2}$ states, which were investigated with the optical double-resonance and the level-crossing methods, as well as with various laser-spectroscopic techniques. The measurements for these states have been reviewed by Arimondo *et al* (1977). Of these states, the $3^2P_{3/2}$ state especially has been extensively studied. A recent quantum-beat measurement yielded the best accuracy obtained so far for the magnetic-dipole and the electric-quadrupole interaction constants (Krist *et al* 1977). The sodium atom, being a light alkali atom with a single electron outside closed shells, is quite suitable for theoretical calculations. Detailed many-body calculations for the 3^2P state have been performed by Lindgren and co-workers (Garpman *et al* 1975, Lindgren *et al* 1976).

The first precision HFS measurement of an excited sodium S state was performed by Liao *et al* (1973) using cascade-RF spectroscopy for the $4^2S_{1/2}$ state. The $5^2S_{1/2}$ state was investigated employing step-wise laser excitations (Tsekeris *et al* 1976). Recently, the studies were extended to the 6, 7 and $8^2S_{1/2}$ states by measurements at this laboratory (Lundberg *et al* 1977). In connection with that work, HFS calculations for the S-state sequence were also performed using many-body perturbation theory. By including polarisation, correlation, and relativistic effects an agreement between theory and experiment to within 1·5% could be obtained. A corresponding study for the sequence of P states is even more interesting as there is also a quadrupole interaction, in addition to the dipole interaction, present in the S sequence. In the evaluation of nuclear quadrupole moments of alkali isotopes, the quadrupole interactions in sequences of $^2P_{3/2}$ states have been studied. So called Sternheimer correction factors,

describing the closed-shell anti-shielding of the quadrupole moment, were frequently employed in such studies (see e.g. Belin and Svanberg 1971). A more general treatment was proposed by Lindgren (1975) and employed by Belin *et al* (1976) for the evaluation of the quadrupole moment of ^{87}Rb from P- and D-state data. A thorough analysis of the quadrupole interaction for ^{23}Na has been hampered by the lack of data for the higher P states. To improve upon this situation we have extended P-state HFS measurements for this atom. Very recently, results for the 4 and $5^2P_{1/2}$ states were presented (Grundevik and Lundberg 1978), obtained in radio-frequency resonance experiments. In the present paper we report on HFS measurements for the $5^2P_{3/2}$ and $6^2P_{3/2}$ states, using the zero-field HFS quantum-beat method. A partial energy-level diagram, including the discussed states, is given in figure 1.

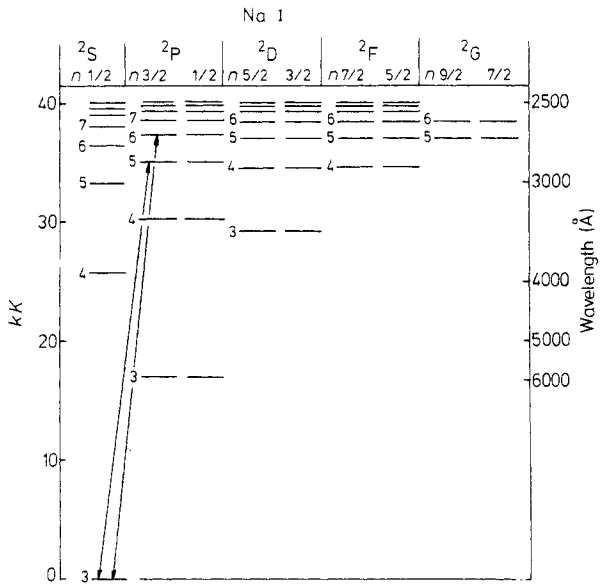

Figure 1. Energy-level diagram for sodium. A wavelength scale for transitions from the ground state is included.

In our quantum-beat measurements we used a frequency-doubled pulsed dye laser, acting on a sodium atomic beam. From a Fourier transform of the beat structure in the time-resolved fluorescence decay curve, the magnetic-dipole and the electric-quadrupole interaction constants, a and b for the studied states, could be determined. In the next section our experimental techniques are presented and in § 3 the different measurements and the data reduction procedure are discussed. Detailed many-body perturbation calculations were performed for all the P states studied so far and the results of these calculations are presented in § 4. Finally, the results are discussed in a concluding section.

2. Experimental technique

The quantum-beat method, used in connection with pulsed-laser excitation, was introduced by Gornik *et al* (1972), studying Zeeman quantum beats. Corresponding

HFS studies were first performed by Haroche *et al* (1973). Subsequently, the quantum-beat method has been used in several investigations, also in connection with step-wise laser excitations (see e.g. Fabre *et al* 1975 and Deech *et al* 1977). This new field was recently reviewed by Haroche (1976).

In our quantum-beat experiments on excited $^2P_{3/2}$ states in ^{23}Na we used the experimental arrangement schematically shown in figure 2. A beam of sodium atoms was formed in a high-vacuum system. The reason for using an atomic beam rather than a gas, enclosed in a sealed-off cell, was the necessity to suppress laser straylight, as the detection had to be performed at the same wavelength as that of the exciting laser light. The beam of sodium atoms was condensed on a liquid-nitrogen trap.

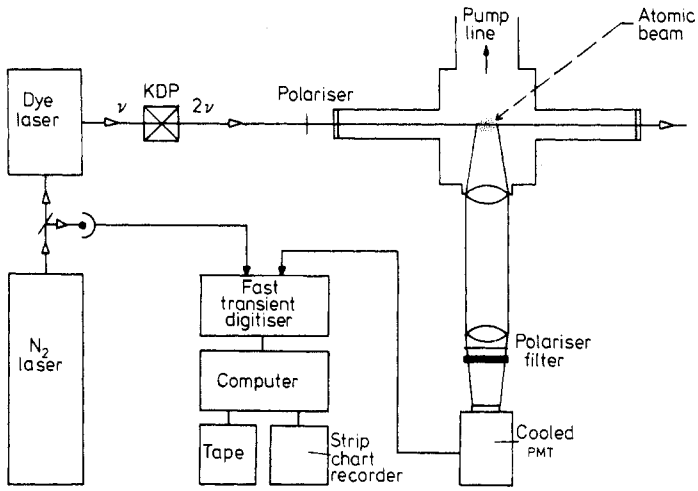

Figure 2. Experimental set-up used in the quantum-beat experiments.

The pulsed laser system consisted of a frequency-doubled dye laser, pumped by a nitrogen laser. The nitrogen laser was a Molectron UV 400 unit, yielding a peak power of 400 kW at 337 nm. This UV light was used to pump a Molectron DL 200 dye laser, which produced 5 ns long pulses with a spectral linewidth of about 0·1 Å. In our experiments the dye C495 was used. The output of the dye laser was focused onto a frequency-doubling KDP crystal, tilted to achieve phase-matching. The UV output pulses had a peak power of about 1 kW and a duration of about 5 ns. The light is partially polarised, but a Polacoat PL 40 UV polariser was used to enhance the polarisation, clearly at the expense of intensity. In order to reduce laser straylight, the laser light was passed in and out of the vacuum system through long tubes. Fluorescence light, released when the excited P-state atoms decay back to the ground state, was detected at the laser wavelength and observed at right angles to the laser and the atomic beam. A Peltier-cooled EMI 9558 QB photomultiplier tube was used for the detection of photons. This detection was performed against the black background of the interior of the vacuum system pumping line. The UV light was isolated using a filter transmitting the proper wavelength. The polarisation of the detected light could be chosen with a UV linear polariser.

The fluorescence photon-intensity distribution following each laser pulse was captured by a Biomation 8100 fast transient digitiser. This device was triggered by a

pulse, derived from a photo-diode, observing part of the nitrogen-laser light pulse. The transient digitiser measured the signal value of every 10 ns interval and the digitised data were transferred into a micro-computer, originally designed for a laser radar system (Nyström 1979). In the micro-computer the optical transients were added to improve the signal-to-noise ratio. The signal stored in the computer memory was read out on a strip-chart recorder and on magnetic tape for further analysis.

The time scale of the fast transient digitiser was calibrated in connection with the measurements by sampling a radio-frequency signal, which was generated by an oscillator, connected to a frequency counter.

3. Measurements and data reduction

Our quantum-beat measurements of the HFS in the 5 and $6^2P_{3/2}$ states were performed in the absence of external fields. The earth's magnetic field was compensated for by Helmholtz-coil systems. In ^{23}Na, which has a nuclear spin of 3/2, a $^2P_{3/2}$ state is split into four HFS levels, characterised by the quantum number F, ranging from 3 to 0. The intervals ΔE between two adjacent levels can be expressed in terms of the magnetic-dipole and the electric-quadrupole interaction constants a and b:

$$\Delta E_{3-2} = 3a + b \qquad \Delta E_{2-1} = 2a - b \qquad \text{and} \qquad \Delta E_{1-0} = a - b$$

(Kopfermann 1958). The selection rules for HFS quantum beats are $\Delta F = \pm 1, \pm 2$, and thus in principle five frequencies can be obtained in the beat spectrum. The possible frequencies are consequently $5a$, $3a+b$, $3a-2b$, $2a-b$ and $a-b$. However, the relative intensities of the beat components vary strongly (Haroche 1976).

In our measurements, the laser light was polarised perpendicularly to the detection direction. When the linear polariser in front of the detector is turned from a position parallel to the laser polarisation to a perpendicular position, the phase of the beats is changed by 180° and the beat amplitudes are decreased by a factor of two. In figure 3 experimental curves for both polariser settings are shown for the $5^2P_{3/2}$ state. The figure also contains the isolated beat structure, obtained by subtracting these two curves. It can be seen clearly that one beat frequency is strongly dominating. This frequency corresponds to the $\Delta E_{3-2} = 3a + b$ interval. When the Fourier transform of an undamped, oscillatory function, extending over only a finite time interval, is to be performed, an apodisation procedure must be applied. The apodisation can be performed by multiplying the curve by a suitable function. The difference signal in figure 3 is damped and therefore includes a 'natural' exponential apodisation which is induced by the decay. By analysing synthetised beat signals with a 'natural' exponential apodisation, simulating our experimental structure, it was found that a strong frequency component could shift a weak, close-by component by up to a fifth of a linewidth. The shift was dependent on the distance in frequency between the peaks and on the phaseshifts between the frequencies. To overcome this problem, apodisation functions besides the exponential one were tested. Before applying the other apodisation functions, the beat signal must be undamped and was therefore divided by a fitted exponential. A cosine-square function with a period of one half of the time interval used was found to give the smallest frequency shifts. It also provided better frequency resolution but still very low oscillations beside the main peak. The smaller peaks in the spectrum were still somewhat shifted in frequency. To improve the accuracy further, the frequency component corresponding to the strongest peak in the Fourier transform

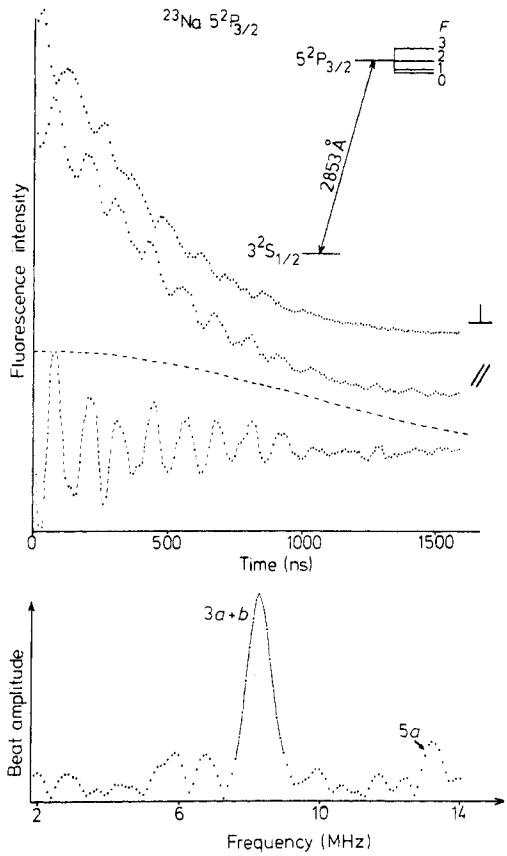

Figure 3. Illustration of measurements for the $5^2P_{3/2}$ state. The upper two curves show decays featuring quantum beats, obtained for perpendicular and parallel polariser settings, respectively. The difference between these two curves is shown in the middle of the figure. Finally, the Fourier transform, obtained with a cosine-square apodisation function also included in the figure, is shown.

was subtracted from the original beat signal. In a repeated Fourier analysis, the previously mentioned frequency shifts were strongly reduced. The frequency, intensity and phase of the peak to be subtracted were taken directly from the primary Fourier analysis.

The cosine-square function is indicated in the figure together with the difference signal. The Fourier spectrum of the beat signal, apodised with the cosine-square function, is given in the lower part of the figure. In the practical evaluation procedure used, the peak subtraction described earlier was performed once or twice to extract two to four frequencies from each curve.

In figure 4 an experimental curve for the $6^2P_{3/2}$ state is shown. The Fourier transform obtained with a cosine-square apodisation is also given. From a large number of experimental curves, analysed in the way just discussed, we obtained the following results for the HFS constants of the two states:

$$a(5^2P_{3/2}) = 2{\cdot}64(1)\ \text{MHz} \qquad b(5^2P_{3/2}) = 0{\cdot}38(3)\ \text{MHz}$$

$$a(6^2P_{3/2}) = 1{\cdot}39(1)\ \text{MHz} \qquad b(6^2P_{3/2}) = 0{\cdot}21(2)\ \text{MHz}.$$

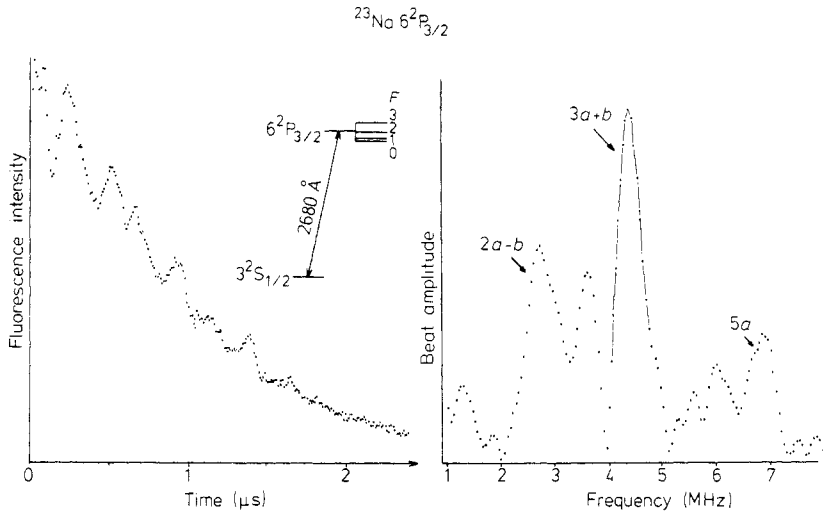

Figure 4. Experimental curve for the $6^2P_{3/2}$ state measured for parallel polariser settings. The cosine-square-apodised Fourier transform is also shown.

The quoted error bars comprise the statistical and the calibration uncertainties as well as the estimated maximum error in the frequency extraction procedure.

4. Theoretical calculations

In the effective-operator formalism for the hyperfine interaction, the magnetic-dipole constant a can be expressed in terms of three radial parameters $\langle r^{-3}\rangle_i$, whereas the quadrupole constant b can be expressed using a single parameter $\langle r^{-3}\rangle_q$ (Lindgren and Rosén 1974):

$$a(^2P_{1/2}) = Cg_I(\tfrac{4}{3}\langle r^{-3}\rangle_l + \tfrac{4}{3}\langle r^{-3}\rangle_{sd} - \tfrac{1}{3}\langle r^{-3}\rangle_c)$$

$$a(^2P_{3/2}) = Cg_I(\tfrac{2}{3}\langle r^{-3}\rangle_l - \tfrac{2}{15}\langle r^{-3}\rangle_{sd} + \tfrac{1}{3}\langle r^{-3}\rangle_c)$$

$$b(^2P_{3/2}) = DQ\langle r^{-3}\rangle_q.$$

Here g_I and Q are the nuclear g factor (proportional to the magnetic moment) and the nuclear quadrupole moment, respectively. $\langle r^{-3}\rangle_l$, $\langle r^{-3}\rangle_{sd}$ and $\langle r^{-3}\rangle_c$ are the radial parameters for the orbital, spin-dipole and contact parts of the interaction. C and D are constants with the numerical values 95·41 and 93·99, respectively, if the interaction constants are given in MHz, the $\langle r^{-3}\rangle$ parameters in atomic units and g_I and Q in nuclear magnetons and barns, respectively.

The goal for a theoretical calculation of atomic hyperfine structure is to get reliable values for the electronic $\langle r^{-3}\rangle$ parameters. We have calculated these parameters for the ^2P states studied so far using many-body perturbation techniques. The calculations are based on a diagrammatic perturbation expansion of effective operators, as described by Garpman *et al* (1975) and Lindgren *et al* (1976), who have studied the 3^2P state of sodium.

The starting point for the calculations is a restricted Hartree–Fock (HF) model for the Na^+ ion. The presence of the valence p electron causes a polarisation of the core.

This effect is studied by solving inhomogeneous single-particle equations. By means of an iterative procedure the core polarisation effects are included to infinite order (Garpman *et al* 1976). This is an alternative way of solving the unrestricted Hartree–Fock equations. Lowest-order correlation effects are studied in a similar way, by solving inhomogeneous two-particle equations, as described by Garpman *et al* (1975). Important higher-order correlation effects are included by modifying the orbitals to approximate Brueckner (natural) orbitals (Lindgren *et al* 1976). The many-body calculations described here are all non-relativistic. The influence of relativity can be estimated using correction factors, calculated by Rosén and Lindgren (1972).

The results of our calculations of radial parameters are given in table 1. The parameter values are calculated employing Hartree–Fock as well as Brueckner (natural) orbitals as a basis set. The zeroth-order (central-field) values, the values including polarisation effects to all orders and, finally, values also including correlation effects, are given separately in the table. As the g_I factor for the ^{23}Na nucleus is known with a high precision ($g_I = 1{\cdot}478\ \mu_N$), the results, with regards to the magnetic-dipole interaction, can also be presented as a factors, using the formulae given above. On the other hand, the electric quadrupole moment Q is not well known, but should rather be determined in this study. Therefore the results of the quadrupole-interaction calculation can only be given as normalised interaction constants b/Q. In table 2 we give theoretical values for a and b/Q. In the first two columns, marked HF, the zeroth-order values obtained with the Hartree–Fock basis (*the* Hartree–Fock values) are given. In the next two columns the values obtained by including polarisation effects to all orders, using the HF basis, are presented. These values are, as mentioned above, identical to those that would have been obtained in an unrestricted HF calculation and the difference between these values and the restricted HF values is, in the customary language, *the* polarisation effect. Finally, values including both the polarisation and the major correlation effects, calculated using the Brueckner orbital basis, are given. Thus,

Table 1. Theoretical values for the radial parameters of the 3^2P–6^2P states of Na using many-body perturbation theory.

		Hartree–Fock basis				'Natural orbital' basis			
State		$\langle r^{-3}\rangle_l$	$\langle r^{-3}\rangle_{sd}$	$\langle r^{-3}\rangle_c$	$\langle r^{-3}\rangle_q$	$\langle r^{-3}\rangle_l$	$\langle r^{-3}\rangle_{sd}$	$\langle r^{-3}\rangle_c$	$\langle r^{-3}\rangle_q$
3^2P†	A‡	0·1674	0·1674	—	0·1674	0·1921	0·1921	—	0·1921
	B	0·2175	0·2263	0·0371	0·2617	0·2501	0·2607	0·0437	0·2953
	C	0·2338	0·2430	0·0111	0·2718	0·2398	0·2496	0·0125	0·2794
4^2P	A	0·0553	0·0553	—	0·0553	0·0624	0·0624	—	0·0624
	B	0·0718	0·0747	0·0117	0·0829	0·0811	0·0845	0·0134	0·0923
	C					0·0777	0·0809	0·0033	0·0874
5^2P	A	0·0246	0·0246	—	0·0246	0·0276	0·0276	—	0·0276
	B	0·0319	0·0332	0·0051	0·0364	0·0358	0·0374	0·0058	0·0403
	C					0·0343	0·0358	0·0014	0·0382
6^2P	A	0·0130	0·0130	—	0·0130	0·0145	0·0145	—	0·0145
	B	0·0168	0·0175	0·0027	0·0191	0·0188	0·0197	0·0030	0·0211
	C					0·0181	0·0188	0·0007	0·0200

† The results obtained for the 3^2P state are almost identical with those already calculated by Lindgren *et al* (1976).

‡ A, zeroth order; B, including polarisation to all orders; C, including polarisation and correlation.

Table 2. Theoretical values for the dipole interaction constant a (MHz) and the normalised quadrupole interaction b/Q (MHz b^{-1}). Experimental values for the constants a and b (MHz) are also included.

State	HF		HF + polarisation		HF + correlation		Experiment	
	a	b/Q	a	b/Q	a	b/Q	a	b
$3^2P_{3/2}$	12·59	15·78	17·94	24·59	18·44	26·26	18·64(6)[a]	2·77(6)[a]
$3^2P_{1/2}$	62·96		81·71		91·45		94·3(1)[b]	
$4^2P_{3/2}$	4·16	5·20	5·89	7·79	5·94	8·21	6·02(6)[b]	0·97(6)[b]
$4^2P_{1/2}$	20·82		27·01		29·68		30·4(5)[c]	
$5^2P_{3/2}$	1·85	2·31	2·61	3·43	2·62	3·59	2·64(1)[d]	0·38(3)[d]
$5^2P_{1/2}$	9·26		12·01		13·12		13·3(2)[c]	
$6^2P_{3/2}$	0·98	1·36	1·38	1·80	1·38	1·88	1·39(1)[d]	0·21(2)[d]
$6^2P_{1/2}$	4·89		6·34		6·90			

[a] Krist *et al* (1977).
[b] Values tabulated by Arimondo *et al* (1977).
[c] Grundevik and Lundberg (1978).
[d] This work.

the values in table 2 are based on the first two lines in the left columns and on the third line in the right columns for each state in table 1. In table 2 the experimental a and b factors for the 3^2P–6^2P states are also presented.

5. Discussion

In figure 5 we have plotted the ratio between theoretical and experimental values for the dipole interaction constant a in the $^2P_{3/2}$ and $^2P_{1/2}$ sequences. The values given in table 2 have been used. The Hartree–Fock theory gives a rather rough description of the hyperfine structure of the studied P states. The values are about 70% of the experimental ones. By adding polarisation effects to all orders, the theoretical values are increased to more than 96% of the experimental ones for the $^2P_{3/2}$ states and to about 87% for the $^2P_{1/2}$ states. The correlation effects contribute only a few per cent for the lowest and almost nothing for the highest $^2P_{3/2}$ states, but for the $^2P_{1/2}$ states the correlation contribution is as high as 9%. By including the correlation effects, the discrepancies between theoretical and experimental values are reduced to 1% for the $^2P_{3/2}$ states and to about 2% for the $^2P_{1/2}$ states. Relativistic effects are not included, but the correction factors given by Rosén and Lindgren (1972) indicate that the effects are of the magnitude of 1%. The remaining discrepancy might be due to numerical uncertainties, higher-order correlation and genuine three-body effects.

In figure 6 we have plotted values for the quadrupole moment Q of the ^{23}Na nucleus employing the experimental b factors and the theoretical b/Q values, taken from table 2. The values obtained using the HF approach do not yield a consistent value for Q. The inclusion of polarisation effects considerably reduces the evaluated Q value, and a more consistent result is obtained. Correlation effects have a relatively small influence

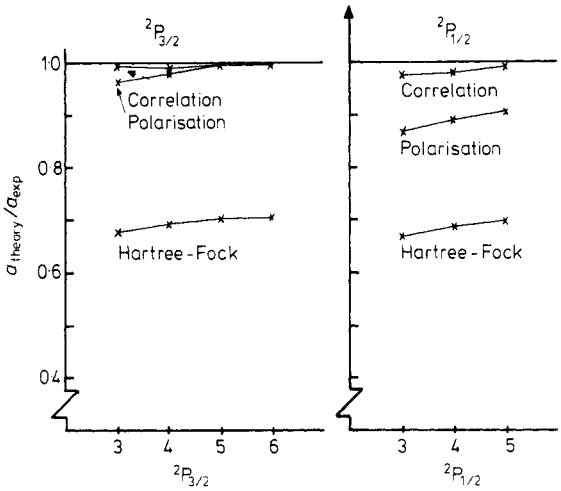

Figure 5. Diagram showing the improved agreement between theoretical and experimental a factors when the contributions from polarisation and correlation effects are added to the Hartree–Fock values.

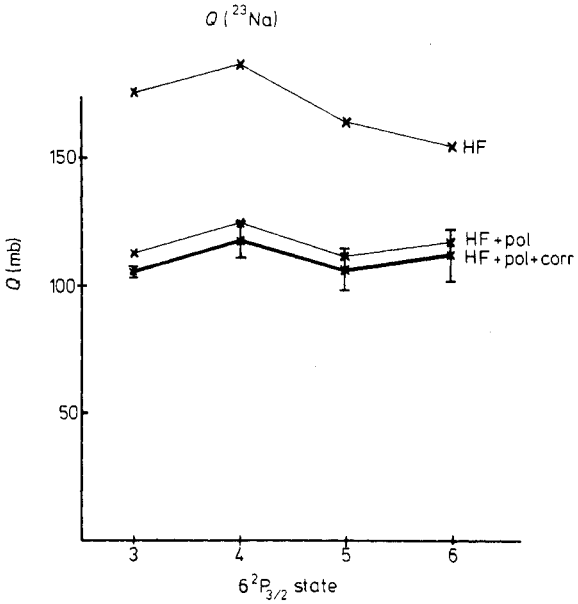

Figure 6. Diagram showing deduced values for the quadrupole moment Q of the ^{23}Na nucleus. The error bars given on the final values take only the uncertainty in the experimental b factors into account.

and only slightly reduce the values. For these last values, error bars are given, taking only the uncertainty in the experimental b factors into account. It seems that the high value obtained for the $4^2P_{3/2}$ state could be due to a slightly high experimental b factor. As a matter of fact, the value used is a weighted mean of two rather differing results, tabulated by Arimondo *et al* (1977). It should also be noted that the b value given for

the $3^2P_{3/2}$ state by these authors, calculated from 14 different investigations, is about 4% higher than that obtained by Krist *et al* (1977). Taking these considerations into account we give as a recommended value $Q(^{23}Na) = 107(5)$ mb for the quadrupole moment.

Acknowledgments

The authors gratefully acknowledge the support of Professor I Lindgren and particularly his advice concerning the theoretical calculations. This work was financially supported by the Swedish Natural Science Research Council.

References

Arimondo E, Inguscio M and Violino P 1977 *Rev. Mod. Phys.* **49** 31–75
Belin G, Holmgren L and Svanberg S 1976 *Phys. Scr.* **13** 351–62
Belin G and Svanberg S 1971 *Phys. Scr.* **4** 269–73
Deech J S, Luypaert R, Pendrill L R and Series G W 1977 *J. Phys. B: Atom. Molec. Phys.* **10** L137–41
Fabre C, Gross M and Haroche S 1975 *Opt. Commun.* **13** 393–7
Garpman S, Lindgren I, Lindgren J and Morrison J 1975 *Phys. Rev.* A **11** 758–81
—— 1976 *Z. Phys.* A **276** 167–77
Gornik W, Kaiser D, Lange W, Luther J and Schulz H H 1972 *Opt. Commun.* **6** 327–8
Grundevik P and Lundberg H 1978 *Z. Phys.* A **285** 231–3
Haroche S 1976 *High-Resolution Laser Spectroscopy, Topics in Applied Physics* vol 13 (Heidelberg: Springer-Verlag)
Haroche S, Paisner J A and Schawlow A L 1973 *Phys. Rev. Lett.* **30** 948–51
Kopfermann H 1958 *Nuclear Moments* (New York: Academic Press)
Krist Th, Kuske P, Gaupp A, Wittman W and Andrä H J 1977 *Phys. Lett.* **61A** 94–6
Liao K H, Gupta R and Happer W 1973 *Phys. Rev.* A **8** 2811–3
Lindgren I 1975 *Atomic Physics* vol 4 (New York: Plenum) pp 747–72
Lindgren I, Lindgren J and Mårtensson A-M 1976 *Z. Phys.* A **279** 113–25
Lindgren I and Rosén A 1974 *Case Studies in Atomic Physics* **4** 93–298
Lundberg H, Mårtensson A-M and Svanberg S 1977 *J. Phys. B: Atom. Molec. Phys.* **10** 1971–8
Nyström K 1979 *Göteborg Institute of Physics Reports* GIPR-178
Rosén A and Lindgren I 1972 *Phys. Scr.* **6** 109–21
Tsekeris P, Liao K H and Gupta R 1976 *Phys. Rev.* A **13** 2309–10